Energy, Mines and Resources Canada | Énergie, Mines et Ressources Canada

CANMET

Canada Centre for Mineral and Energy Technology | Centre canadien de la technologie des minéraux et de l'énergie

DEGRADATION OF MAGNESIA-CARBON BRICKS IN ARGON ATMOSPHERE AT HIGH TEMPERATURE

S.S.B. Wang, D.H.H. Quon and J. Aota
Mineral Processing Laboratory

December 1987

Project: 30.29.05
Electrodes and Refractories for Steelmaking

This document is an unedited internal report prepared primarily for discussion and documentation purposes. It does not represent a final expression of the opinion of the Canada Centre for Mineral and Energy Technology (CANMET)

Ce document est un rapport provisoire non-révisé et rédigé principalement pour fin de discussion et de documentation internes. Il ne représente nullement l'expression définitive de l'opinion du Centre canadien de la technologie des minéraux et de l'énergie (CANMET)

21 pp

MINERAL SCIENCES LABORATORIES
DIVISION REPORT MSL 87-152 (IR)

MICROMEDIA

DEGRADATION OF MAGNESIA-CARBON BRICKS IN ARGON ATMOSPHERE AT HIGH TEMPERATURE

by

S.S.B. Wang*, D.H.H. Quon* and J. Aota+

ABSTRACT

The structural and chemical profiles of four types of MgO-C bricks in contact with high and low calcium slags at 1650°C in an argon atmosphere were examined. The corrosion resistance of the bricks is strongly dependent on the slag composition and decreases with increasing slag basicity due to the formation of calcium carbide.

Keywords: refractories, magnesia-carbon bricks, corrosion resistance of magnesia-carbon bricks.

---

*Research Scientist and +Physical Scientist, Ceramic Section, Mineral Processing Laboratory, Mineral Sciences Laboratories, CANMET, Energy, Mines and Resources Canada.

DÉGRADATION DE BRIQUES AU MAGNÉSIUM-CARBONE, À HAUTE TEMPÉRATURE, DANS UNE ATMOSPHÈRE D'ARGON

par

S.S.B. Wang*, D.H.H. Quon* et J. Aota+

RÉSUMÉ

On a étudié les profils structurel et chimique de quatre différentes briques MgO-C, en contact avec des laitiers dont le contenu en calcium était soit élevé ou faible, à une température de 1 650°C, dans une atmosphère d'argon. La résistance des briques à la corrosion dépend fortement de la composition des laitiers. Cette résistance diminue à mesure que la basicité des laitiers augmente en raison de la formation de carbure de calcium.

Mots-clé : Réfractaires, briques au magnésium-carbone, corrosion
Résistance des briques au magnésium-carbone.

---

*Chercheur scientifique et +Physicien, Section des céramiques, Laboratoire de traitement des minéraux, Laboratoires des sciences minérales, CANMET, Énergie, Mines et Ressources Canada.

INTRODUCTION

Magnesia-carbon (MgO-C) bricks were used mainly in converter lining and electric arc furnaces prior to 1978. Its usage has increased significantly in recent years for other steel making applications. Traditionally, rebonded fused grain chrome magnesia bricks have been used at the slagline and fused cast chrome-magnesia blocks in the hot spots of secondary steelmaking ladles. These bricks are now being replaced by the magnesia-carbon bricks. The excellent performance of MgO-C refractories is the result of various outstanding properties, including high thermal conductivity, good thermal shock, corrosion and erosion resistance as well as its high refractoriness. There are several types of magnesia-carbon bricks with low to high carbon content. One of the major disadvantages of magnesia carbon brick is its low oxidation resistance and decarbonization at the hot face during service, which makes it susceptible to slag attack. To overcome this problem there is continuing research aimed at a better understanding of the conditions under which these degradation processes can be avoided. As part of the continuing effort to examine the refractory degradation in steelmaking, this study is intended to evaluate the performance of MgO-C bricks in contact with secondary steelmaking slags and to assess their applicability in argon environments in the ladle. A similar study was conducted in CANMET on the performance of MgO-C bricks in contact with slags under vacuum (1).

GENERAL CHARACTERISTICS OF MAGNESIA-CARBON BRICKS

Prior to 1978, the MgO-C brick was generally composed of sintered magnesia, and amorphous graphite bonded by coal tar pitch. The second generation of MgO-C bricks was characterized by high carbon levels (10-30%) achieved by the use of natural graphite. Orientation of the flakes in a direction perpendicular to the direction of pressing resulted in an increased resistance to oxidation (often the principal source of degradation). At about the same time, magnesia-carbon products with improved erosion resistance were introduced. The increased erosion resistance was achieved by introduction of resin bonds and fused magnesia grains. Mikami and Martnet classified these bricks into four different categories according to the carbon content as follows (2):

1) 4-5% class - used mainly in basic oxygen furnaces or convertors;
2) 8% class - extensively used in electric arc furnaces in the U.S.A.;
3) 13% class - the carbon levels ranging from 12 to 16%;
4) 18-25% class - highest carbon level is nominally about 20% to as high as 30%, used extensively in electric arc furnaces in Japan.

The pitch-bonded, sintered magnesia brick with 20% carbon of which its entire matrix is composed of flake graphite, carbon black and pitch has been used successfully in electric arc furnaces (2).

The use of MgO-C bricks in basic oxygen furnaces has been reported by other investigators (3-12). It was found that the

carbon and magnesia are incompatible at 1600°C due to the reduction of magnesia and the oxidation of carbon causing modification of the micro-structure of the brick. Some investigators reported the existence of a dense MgO zone developed at or near the hot face of the brick, resulting from the reduction of the MgO and vaporization of Mg with subsequent reoxidation and precipitation of MgO. The newly formed MgO zone acted as a barrier to slag penetration (11). In vacuum at high temperatures, sublimation of Mg and graphite occurred, with gaseous Mg being removed by the vacuum from the furnace, preventing the formation of the dense MgO layer at or near the hot face as reported in the basic oxygen furnace (1).

EXPERIMENTAL

Materials

Materials used for this work were obtained from the Atlas Steels Company, Welland, Ontario. A list of the various types of MgO-C bricks and their physical and chemical properties are given in Table 1.

Characterization

The microstructures of the unused and test bricks were characterized principally by scanning electron microscopy (SEM). Semi-quantitative analysis of the compositional change of the test bricks resulting from the interaction with different slags at 1650°C was determined using energy dispersive X-ray analysis (EDXR).

X-ray diffraction (XRD) was used to determine the phases resulting from the brick-slag interaction at the slag-brick interface.

Slag Resistance Test

The slag resistance of the bricks was conducted at 1650°C for three hours in an Astro furnace*. The furnace was initially evacuated to a pressure of about 5 micron and then filled with argon gas at 83 kpa (12psi.) The test procedure (cup test) has been described previously (1). The slag compositions are given in Table 2.

---

*Manufactured by Astro Industries, Inc., Santa Barbara, Calif., U.S.A.

RESULTS

Because carbon content, apparent porosity, and bulk density of the unused bricks are different, it is important to examine their microstructure. A more detailed description of the microstructure of these bricks has been presented by Quon & Bell (1).

Megascopically, the major visual difference in these bricks is the yellowish colour of the grog grains for samples A and B and white colour for samples C and D.

Microstructures for samples A and B are almost identical. The fine-grained periclase is bonded by calcium silicate to form large grog grains and flake graphite dispersed in the groundmass containing fine-grained periclase and the grog periclase grains (Fig. 1). A spinel phase was detected in sample A and EDXR indicated that this phase was rich in Cr, Al and Fe. Spinel phase was also detected in sample B with Mg and Al as principal elements.

Microstructure and elemental distribution maps of sample C are shown in Fig. 2. Again finer-grained periclase in the grog grains are bonded by calcium silicate. In the groundmass, the principal phases are fine-grained periclase and flake graphite with quartz inclusions. Elemental distribution maps indicate the presence of Fe, K, Al, S and P is mainly associated with the graphite flakes.

The microstructure and elemental distribution maps of Mg, Ca, Si, Fe and S for sample D are given in Fig. 3 and 4. The distribution of grog grains and graphite flakes is very similar to sample C. The principal impurities such as Ti, Al, Fe and Si are detected as inclusions in the graphite flakes.

Weight Loss of Samples Heated at 1600°C

It was reported by other investigators (1,8,10,11,12) that during firing of MgO-C bricks in air or in vacuum, a loss of Mg and C components occurred which could be represented by the following decarbonation reaction:

$$MgO(s) + C(s) = Mg(g) + CO(g)$$

The above reaction caused a progressive carbon burnout and magnesia loss, thereby modifying the refractory properties. In order to determine whether a similar reaction mechanism occurs in the argon atmosphere, 2.5 x 2.5 x 2.5 cm MgO-C cubes were cut from the unused bricks and these samples were heat-treated at 1600°C for three hours under argon atmosphere. The weight difference before and after firing was determined and the results indicated that the weight loss of the samples was in the following order: A < B < C < D and having a loss rate of 0.01, 0.03, 0.04 and 0.07 g/min respectively. The cause of the differences in loss in these samples is not readily understood but it may be due to the distribution of magnesia and carbon in the samples. Nevertheless, a loss of constituents occurred for all samples fired in argon atmosphere at high temperatures but at a substantially reduced rate when compared to samples fired in vacuum (1).

Corrosion Resistance of Magnesia-carbon Refractories

Two types of slags having lime to silica ratios (C/S) of 0.96 and 3.13 were used to test the corrosion resistance of these bricks. The experimental conditions were three hours, at 1650°C, in an argon atmosphere.

Corrosion Resistance of Bricks to Slag With C/S = 3.13

For each test, the residual slag in the test cup on cooling to room temperature tended to decrepitate due to the inversion of the dicalcium silcate present in the slag. An acetylene-like smell was detected from the test samples. The fetid smell appears to stem from the reaction of the calcium carbide (CaC_2) with the humid air. The CaC_2 was likely formed by the reaction between calcium oxide in the slag and carbon in the brick at high temperature. In order to detect the CaC_2 phase in the test samples, XRD analysis was conducted. In addition to the diffraction lines corresponding to dicalcium silicate, diffraction lines at 0.27, 0.194, 0.186, 0.166 and 0.137 nm corresponding to calcium carbide were also observed.

SEM micrographs at the slag-brick interface for the test samples were obtained and the slag corrosion resistance of the brick was examined by analysing the various phases formed by the interaction of the brick and slag by EDXR.

The microstructure of brick A at the slag brick interface is shown in Fig. 5. The micrograph shows that the fine periclase grains, which form the grog grains are bonded by a liquid phase with interstitial lamellar or graphite flakes. The elemental distribution of Ca, Mg, and Si in Fig. 5 shows that the calcium aluminium silicate liquid phase is located principally at the grain boundaries of the fine periclase grains within the grog grains. The slag penetration follows the grain boundaries of the periclase and the basal cleavages of the flake graphite.

Very similar microstructures were also developed at the slag brick interface for brick B, as shown in Fig. 6. Elemental distribution of Ca, Mg, Si, and Al at the slag brick interface indicates that very fine-grained periclase is being dissolved by the slag. The grog grains at the interface appear relatively

intact without much dissolution caused by the slag penetration. The high slag corrosion resistance of the graphite flakes which form slag resistance barrier at the interface can be readily seen in the elemental distribution maps and micrograph.

Apart from the slight difference in the size of the grog periclase grains for sample C and D as shown in Fig. 7 and 8, the slag corrosion resistance of these two samples are very similar as evidenced by the calcium silicate liquid phase formed at the grain boundaries of the grog and fine periclase grains. Elemental distribution maps for Ca, Mg, Si, Al, Fe and S in the above figures indicate that the slag phase is composed principally of calcium alumino silicate.

Corrosion Resistance of Bricks to Slag With C/S = 0.96

For the tests with low lime slag, decrepitation of the slag was not observed and the fetid smell of acetylene was also absent. This indicated that there was insufficient calcium oxide in the slag to react with silica to form dicalcium silicate or to react with carbon to form CaC_2.

At the slag-brick interface, a partial dissolution of the periclase grains by the slag and penetration of the slag along grain boundaries occurred, as shown in Fig. 9, 10, and 11. The absence of intense slag penetration was observed in areas where graphite flakes were present. A dendritic phase was formed along with a liquid phase in the slag-brick interface.

SEM micrographs and elemental distribution maps for test samples A, B, and D at the slag-brick interface are identical. A typical microstructure with elemental distribution maps for these samples is given in Fig. 9, 10, and 11. The microstructure shows that a very sharp slag-brick interface developed and the slag

penetration into the brick followed the grain boundaries of the periclase. There are two principal phases formed in the slag as revealed by the elemental distribution maps for Mg, Ca, Si and Al. On cooling, the calcium silicate phase was the first to crystallize from the slag followed by the low melting calcium aluminum silcate phase which was found at the interstices of the calcium silicate.

DISCUSSION AND CONCLUSIONS

The advantage of graphite in MgO-C bricks in retardation of slag penetration in an argon environment has been demonstrated. In argon, the loss of MgO due to the periclase grains being in contact with the carbonaceous material is substantially lower than in vacuum.

Degradation of the bricks is due to direct chemical corrosion of the MgO by the slag; it is restricted to exposed surfaces and proceeds more readily at the less-resistant grain boundaries. The degree of brick degradation depends on the slag composition. In contact with high calcium slag, graphite reacts with calcium oxide to form calcium carbide. The loss of graphite removes the carbon barrier, thus weakening the surface layer and accelerating the degradation of refractory. Degradation of refractory in contact with slag having low lime content is due to dissolution of periclase grains by the slag.

The formation of a dense MgO layer behind the slag-brick interface was not observed for tests conducted in an argon atmosphere, leading to the conclusion that very little Mg evaporation took place under a pressurized argon atmosphere.

ACKNOWLEDGEMENTS

The authors wish to express their thanks to R. Carson, Senior Development Metallurgist of the Atlas Steels Company for supplying the materials necessary for this study. Thanks are also due to J.M. Beaulne and D. Owens of CANMET for their contribution to this work.

REFERENCES

1. Quon, D.H.H. and Bell, K.E., "Performance of magnesia-carbon bricks in vacuum at high temperature" Accepted for publication in the Journal of the Canadian Ceramic Society 1987.

2. Mikami, H.M. and Martinet, J.R. "Carbon-magnesia bricks in electric arc furnace" Refract J 6:25-32; 1980.

3. Nacumu, R.L. and Lalama, S.J. "High carbon-magnesia refractories in basic oxygen steelmaking" Refract J 4:9-14; 1982.

4. Herron, R.H. Beechan, C.R. and Padfield, R.C. "Slag attack on carbon-bearing basic refractories" Bull Am Ceram Soc 46: 1163-1168; 1967.

5. Carniglia, S.C. "Limitations on the internal oxidation reduction reactions in the BOF refractories" Bull Am Ceram Soc 52:160-165; 1973.

6. Park, H.K. and Barrett, L.R. "The corrosion resistance of carbon-containing magnesia refractories in melts" Trans Br Ceram Soc 78: 90-95; 1979.

7. Park, H.K. and Barrett, L.R. "The oxidation of carbon under melts" Trans Br Ceram Soc 78: 26-33; 1979.

8. Nacamu, R.L. and Batchelor, J.D. "Carbon oxidation as a function of BOF texture" Bull Am Ceram Soc 54:647-649; 1975.

9. Cooper, C.F. "Graphite containing refractories" Refract J 2:11-21, 1984.

10. Baker, B.H., Brezny, B. and Shultz, R.L. "The role of carbon in MgO refractories" Bull AM Ceram Soc 54: 665-666; 1975.

11. Pickering, G.D. and Batchelor, J.D. "Carbon-MgO reactions in BOF refractories " Bull Am Ceram Soc 50: 611-614; 1971.

12. Lin, Y-L and Semler, E. "Effect of oxidation-reduction reactions in magnesia-graphite compositions" pp 27-29 in Application of Refractories, published by The American Ceramic Society, May 1985.

Table 1. Chemical and physical properties of the MgO–C bricks

Brick No.	A	B	C	D
Manufactured by	N. American	N. American	Kyushu	Kyushu
Composition,%				
MgO	71.8	72.0	73.2	82.0
C	24.0	18.3	23.8	14.7
Apparent porosity,%	3.5	3.5	4.4	4.0
Bulk density, kg/m^3	2850	2800	2760	2850

Table 2. Compositions of the slags used for the cup test

	CaO	MgO	SiO_2	Fe_2O_3	Al_2O_3	Cr_2O_3	C/S*
S1	60.06	3.68	19.2	——	10.11	0.02	3.13
S2	36.59	12.79	38.15	0.94	10.04	0.43	0.96

*Weight ratio of CaO:SiO_2

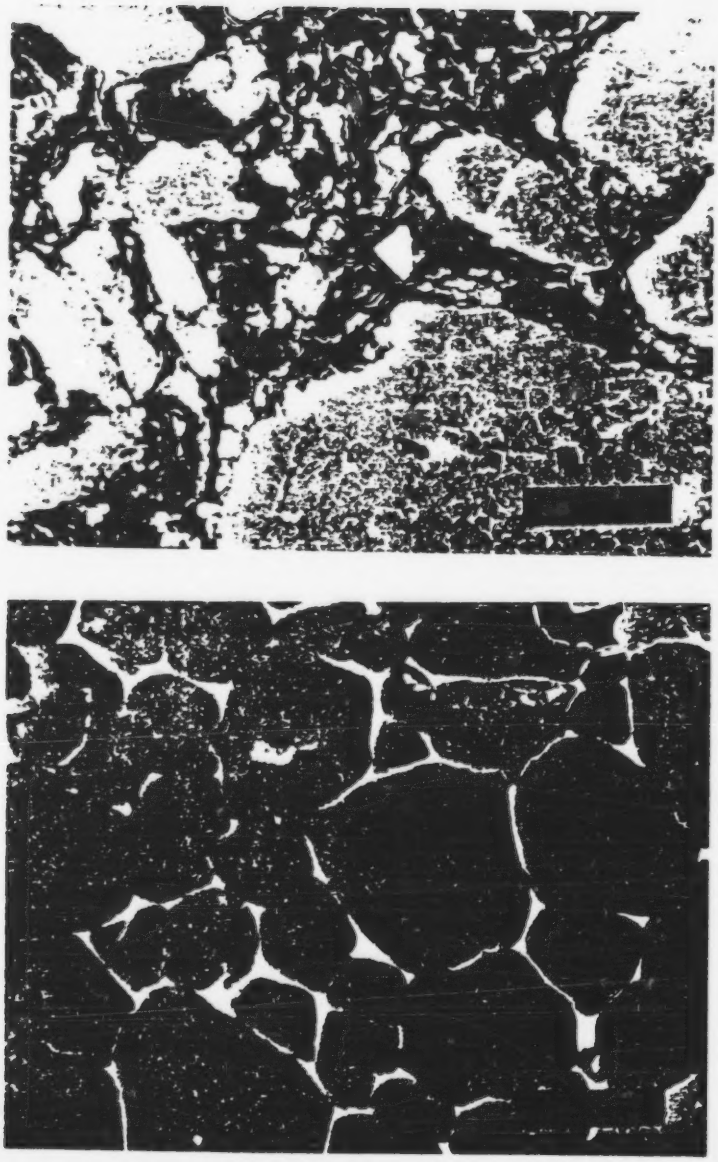

Fig. 1. The microstructure of sample A (1a), and details of the calcium silicate formed at the grain boundaries of the periclase (1b)

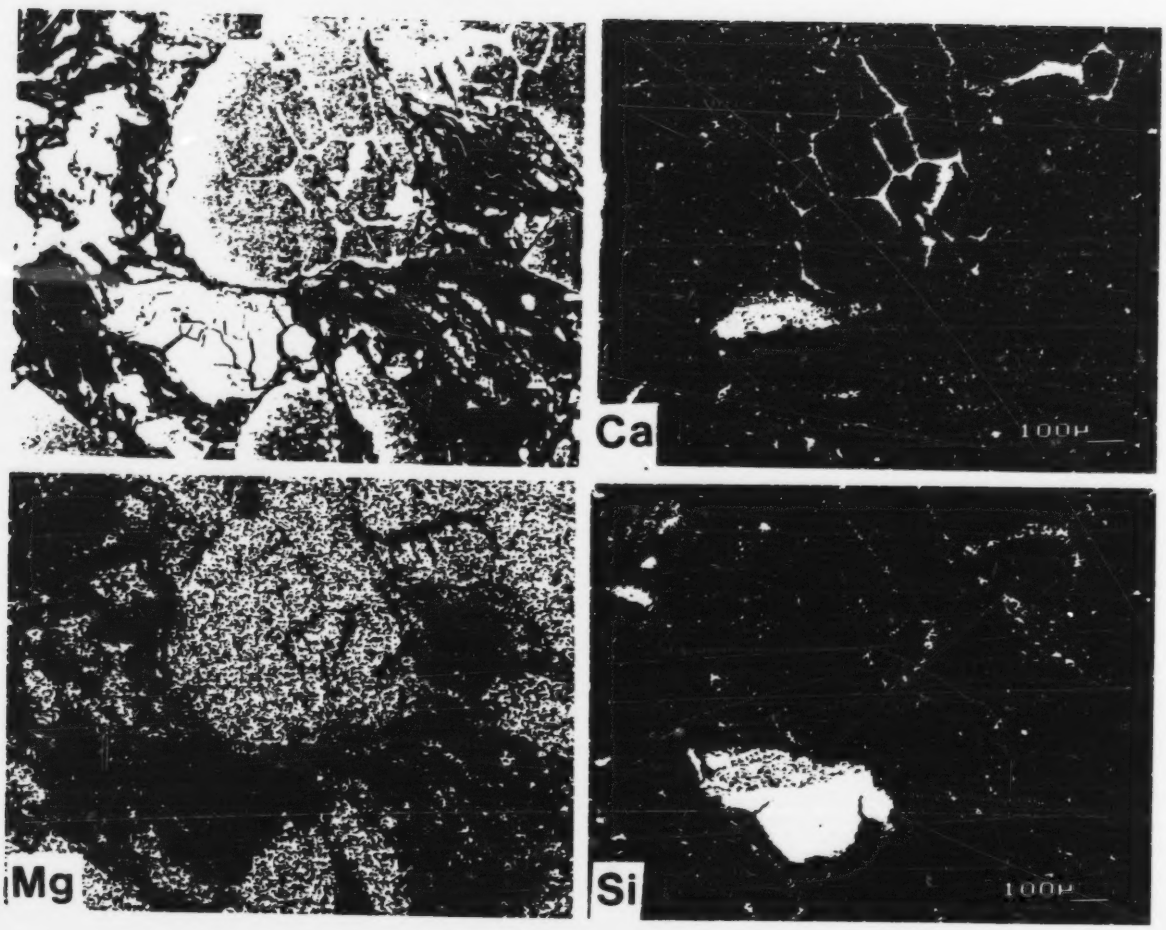

Fig. 2. SEM micrograph and elemental distribution maps of Ca, Mg and Si for sample C

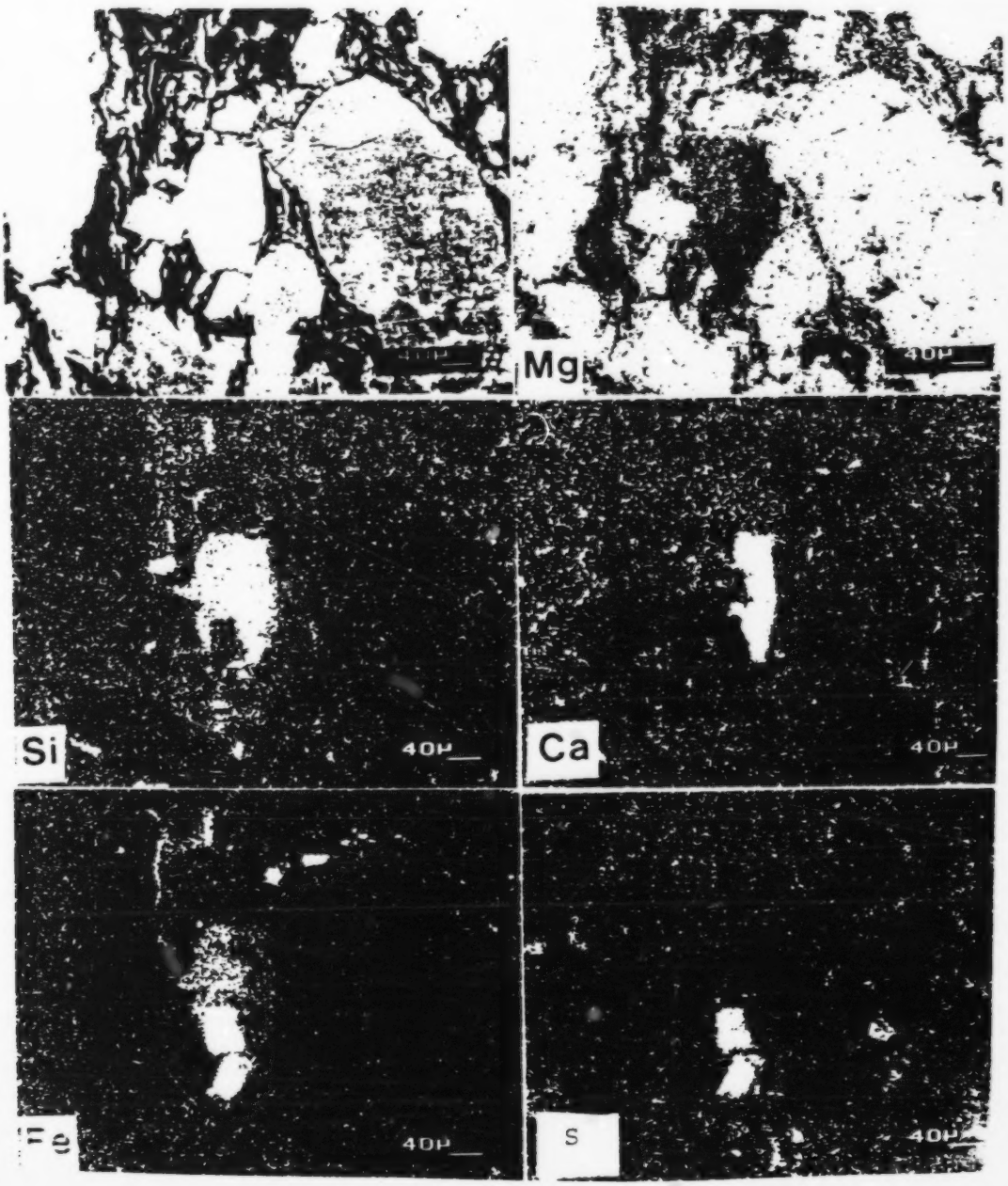

Fig. 3. SEM micrograph and elemental distribution maps of Mg, Ca, Si, Fe and S for unused brick D

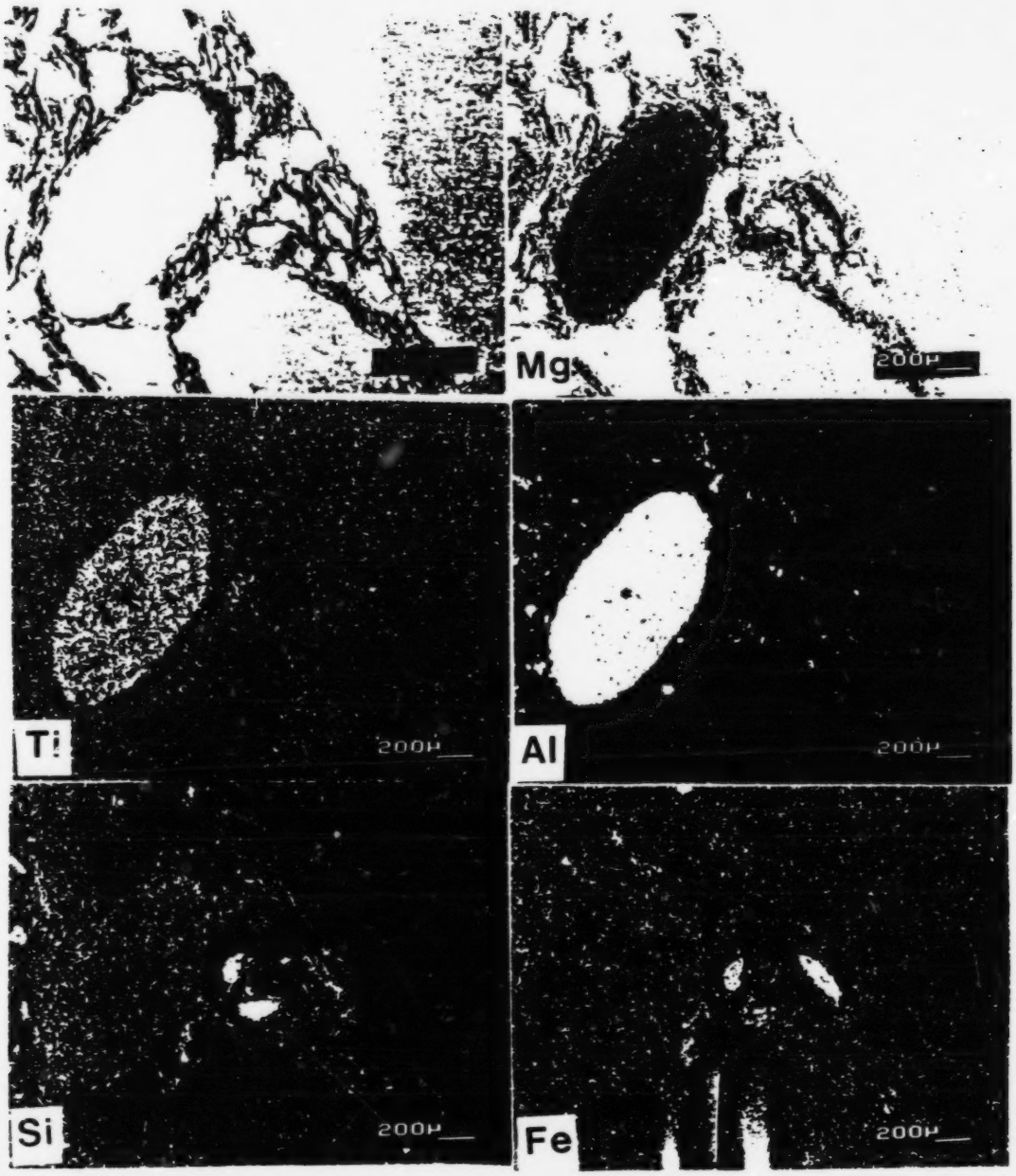

Fig. 4 SEM micrograph and elemental distribution maps of Mg, Ti, Al, Si and Fe for unused brick, D

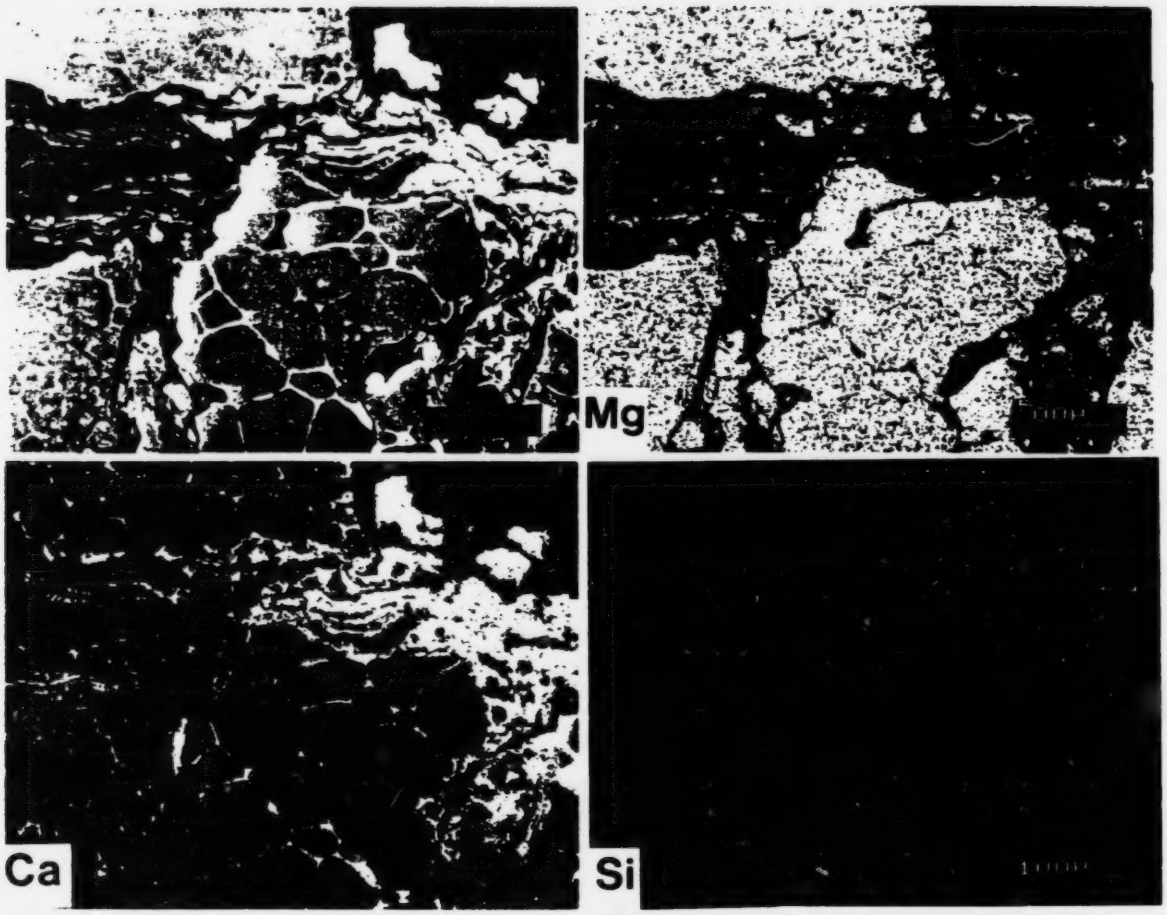

Fig. 5. SEM micrograph and elemental distribution maps of Ca, Mg, and Si for brick A, in contact with slag of C/S = 3.13

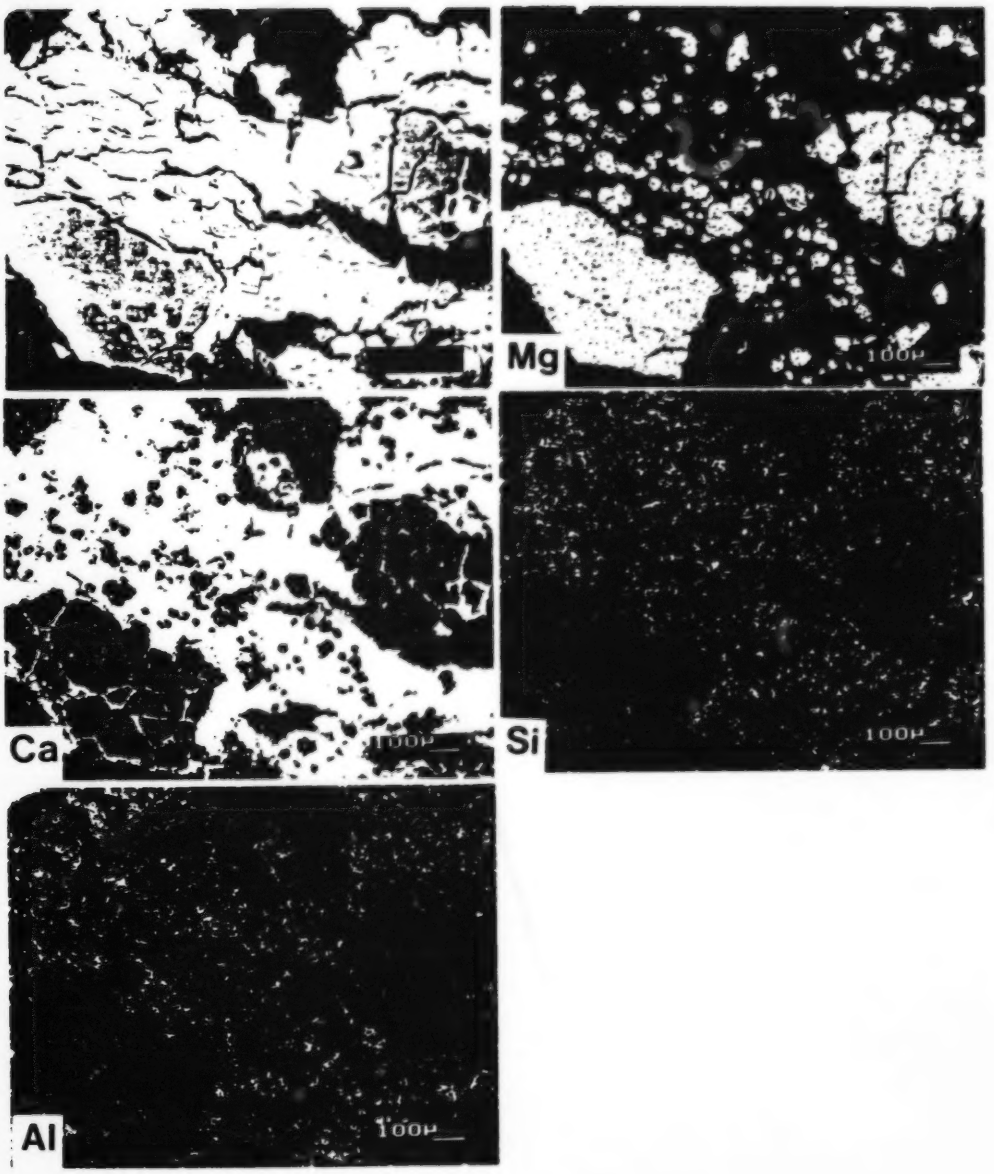

Fig. 6. SEM micrograph and elemental distribution maps of Ca, Al, Mg, and Si for brick B in contact with slag of C/S = 3.13

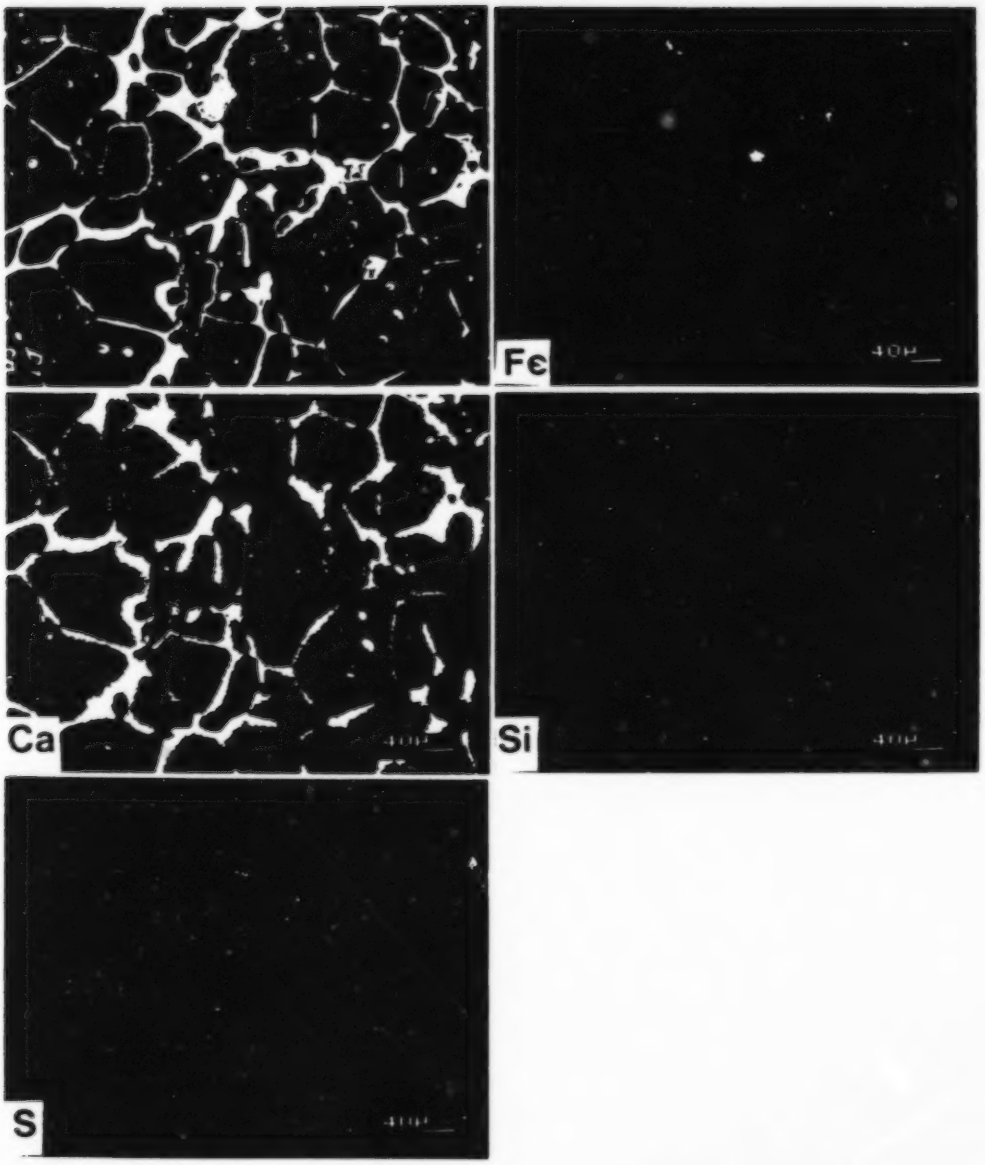

Fig. 7. SEM micrograph and elemental distribution maps of Ca, Fe, Si and S for brick C in contact with slag of C/S = 3.13

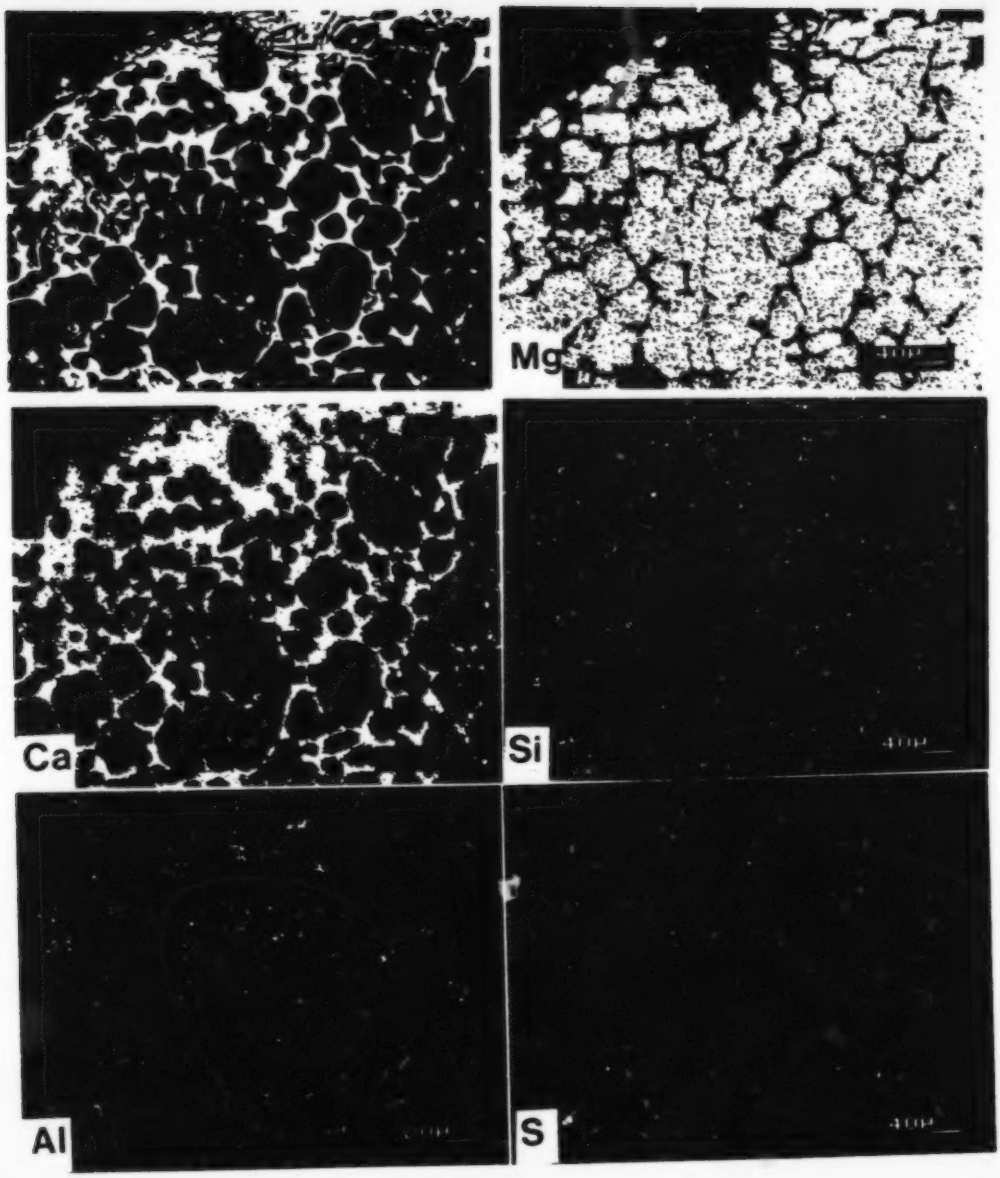

Fig. 8. SEM micrograph and elemental distribution maps of Ca, Mg, Si, Al and S for brick D in contact with slag of C/S = 3.13

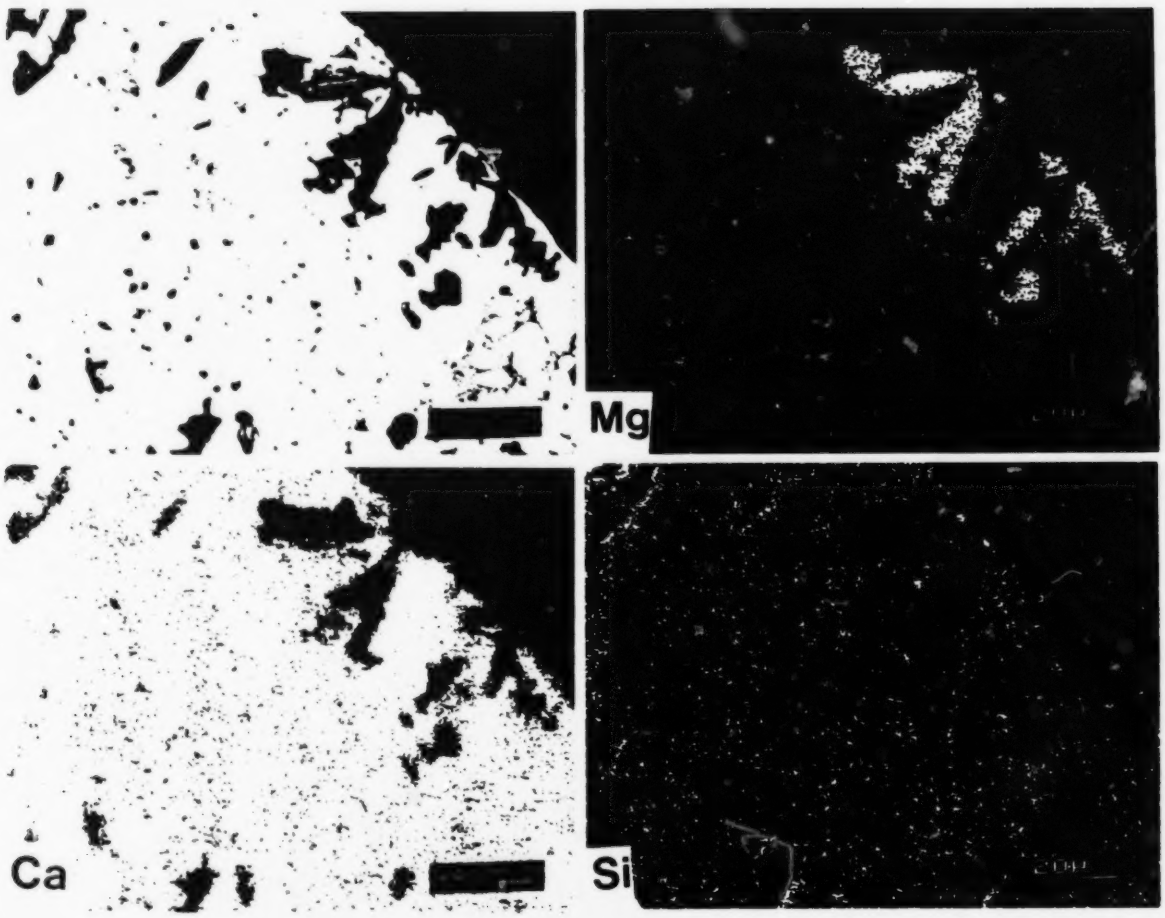

Fig. 9. SEM micrograph and elemental distribution maps of Ca, Mg and Si for brick A in contact with slag of C/S = 0.96

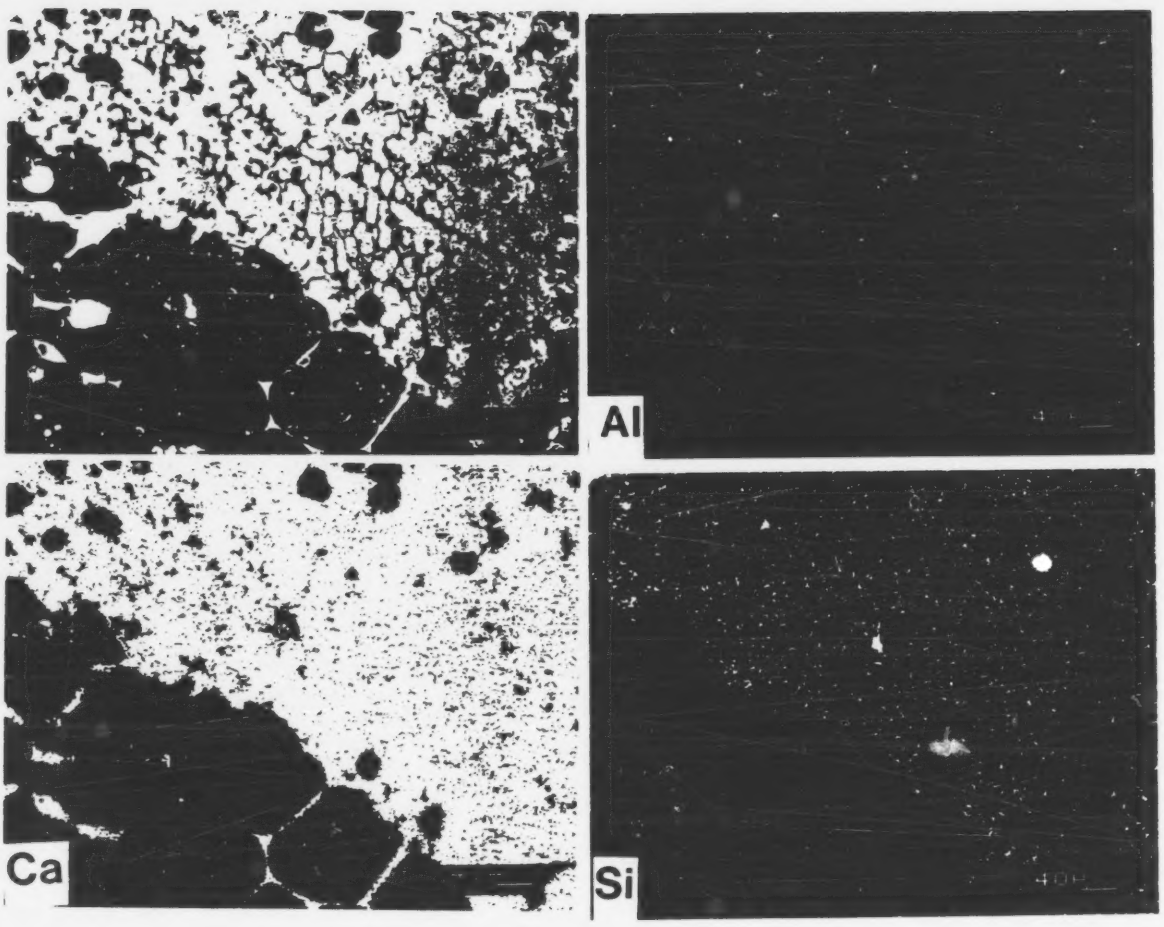

Fig. 10. SEM micrograph and elemental distribution maps of Ca, Mg and Si for brick B in contact with slag of C/S = 0.96

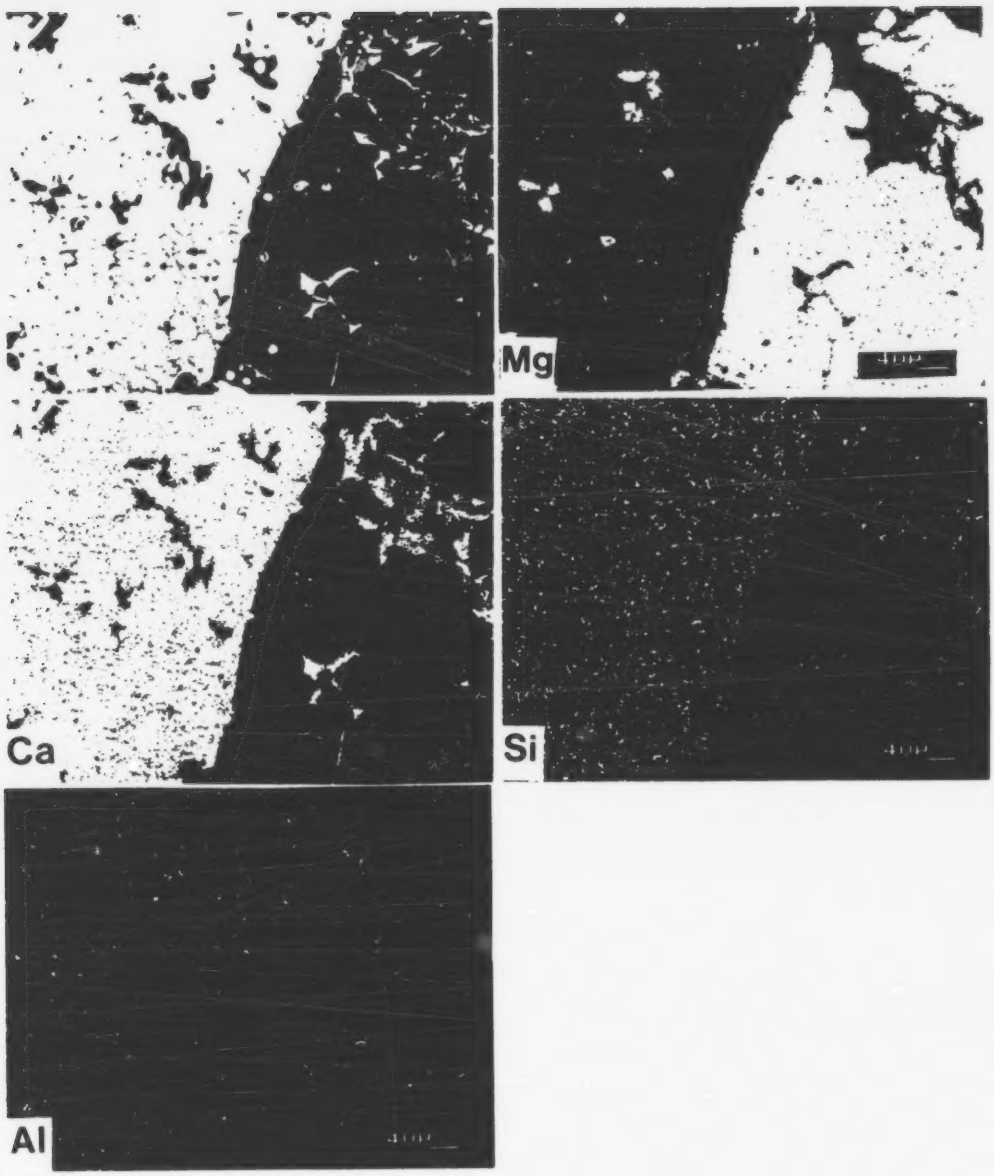

Fig. 11. SEM micrograph and elemental distribution maps of Ca, Mg, Si and Al for brick D in contact with slag of C/S = 0.96